can explain the solution dynamics of all microtubule systems at all times and under all conditions.

ACKNOWLEDGMENTS

We thank Jeanne Ellermeier and Bonnie Neighbors for their excellent technical assistance. We gratefully acknowledge the logistical support provided by the staff of the Division of Polar Programs of the National Science Foundation, by the personnel of ITT Antarctic Services, Inc., and by the captains and crews of *R/V Polar Duke*.

REFERENCES

Bradford, M. M. (1976) *Anal. Biochem. 72*, 248–254.
Caplow, M., Shanks, J., & Brylawski, B. P. (1986) *J. Biol. Chem. 261*, 16233–16240.
Cote, R. H., & Borisy, G. G. (1981) *J. Mol. Biol. 150*, 577–602.
Detrich, H. W., III, & Overton, S. A. (1986) *J. Biol. Chem. 261*, 10922–10930.
Detrich, H. W., III, Jordan, M. A., Wilson, L., & Williams, R. C., Jr. (1985) *J. Biol. Chem. 260*, 9479–9490.
Detrich, H. W., III, Prasad, V., & Ludueña, R. F. (1987) *J. Biol. Chem. 262*, 8360–8366.
Farrell, K. W., & Jordan, M. A. (1982) *J. Biol. Chem. 257*, 3131–3138.
Farrell, K. W., Jordan, M. A., Miller, H. P., & Wilson, L. (1987) *J. Cell Biol. 104*, 1035–1046.
Gaskin, F., Cantor, C. R., & Shelanski, M. L. (1974) *J. Mol. Biol. 89*, 737–758.
Horio, T., & Hotani, H. (1986) *Nature (London) 321*, 605–607.
Hotani, H., & Horio, T. (1988) *Cell Motil. Cytoskel. 10*, 229–236.
Kirschner, M. W. (1980) *J. Cell Biol. 86*, 330–334.
Kirschner, M., & Mitchison, T. (1986) *Cell 45*, 329–342.
Kristofferson, D., Mitchison, T., & Kirschner, M. (1986) *J. Cell Biol. 102*, 1007–1019.
Margolis, R. L., & Wilson, L. (1978) *Cell 13*, 1–8.
Mitchison, T., & Kirschner, M. (1984) *Nature (London) 312*, 237–242.
Rothwell, S. W., Grasser, W. A., & Murphy, D. B. (1986) *J. Cell Biol. 102*, 619–627.
Rothwell, S. W., Grasser, W. A., Baker, H. N., & Murphy, D. B. (1987) *J. Cell Biol. 105*, 863–874.
Walker, R. A., O'Brien, E. T., Pryer, N. K., Soboeiro, M. F., Voter, W. A., Erickson, H. P., & Salmon, E. D. (1988) *J. Cell Biol. 107*, 1437–1448.
Williams, R. C., Jr., & Detrich, H. W., III (1986) *Ann. N.Y. Acad. Sci. 466*, 436–439.
Williams, R. C., Jr., & Rone, L. A. (1988) *Protoplasma 145*, 200–203.
Williams, R. C., Jr., Correia, J. J., & DeVries, A. L. (1985) *Biochemistry 24*, 2790–2798.
Wilson, L., Snyder, K. B., Thompson, W. C., & Margolis, R. L. (1982) *Methods Cell Biol. 24*, 159–169.
Zeeberg, B., Reid, R., & Caplow, M. (1980) *J. Biol. Chem. 255*, 9891–9899.

Discovery and Mapping of Discrete Binding Sites on Nucleosome Core Particles for a Photoaffinity Derivative of Spermine†

James E. Morgan,‡ Catharine C. Calkins,§ and Harry R. Matthews*

Department of Biological Chemistry, School of Medicine, University of California, Davis, California 95616

Received December 6, 1988; Revised Manuscript Received March 10, 1989

ABSTRACT: A polyamine photoaffinity analogue, (azidonitrobenzoyl)spermine (ANB-spermine), has been synthesized and characterized. Thermal denaturation studies showed that ANB-spermine interacted noncovalently with nucleosome core particles similarly to naturally occurring polyamines carrying the same charge (+3). Photoaffinity labeling of core particles with ANB-spermine resulted in covalent binding of about 3% to the DNA and a similar amount to the histones. The locations of covalent binding to DNA were determined by exonuclease protection using T4 DNA polymerase–exonuclease. There was significant nonspecific binding and 7 discrete sites of preferred binding: at the 3′ end and centered at positions 15, 36, 56, 86, 109 and 130 bases from the 3′ end. A possible site at the 5′ end could not be determined by this technique. The sites were roughly symmetrical about the center of the DNA molecule, indicating labeling of both strands of the helix. The sites were offset from DNase I nicking sites by 3–5 bases, indicating that they are not on the exterior of the core particle. The sites occurred in the core particle where the two turns of the DNA supercoil are closely apposed, with a conspicuous gap where there is a single turn of the supercoil. By use of a CTAB/SDS–protein two-dimensional gel system, it was found that histones were labeled to differing extents, with H3 = H2B > H2A > H4. Partial tryptic digestion showed that the histones were labeled mainly (73–80%) in the central, globular regions. The data indicate that ANB-spermine and, presumably, the naturally occurring polyamines bind both in a nonlocalized fashion and at specific sites on the nucleosome core particle.

Chromatin undergoes major alterations during the transitions from the inactive to the potentially active to the actively transcribed state (Reeves, 1988; Garrard et al., 1988) and during replication (DePamphilis & Wassarman, 1980; Annunziato & Seale, 1983). These alterations must fundamentally open up the compact form of bulk chromatin and allow the bases of the DNA to become accessible to base pairing with the nascent RNA or DNA. Acetylation of histones has been correlated with transcription and replication (Allfrey et al., 1964; Allfrey, 1977; Allegra et al., 1987; Matthews, 1988; Hebbes et al., 1988). Experiments have shown that histone

† This project was supported by the National Science Foundation (DCB-87 05378).

* Address correspondence to this author.
‡ Supported in part by a National Science Foundation Graduate Student Fellowship. Present address: Department of Pharmacology, Stanford University School of Medicine, Stanford, CA 94305.
§ Present address: Collagen Corp., Palo Alto, CA 94303.

0006-2960/89/0428-5095$01.50/0

acetylation reduces the stability of nucleosome core particles to thermal denaturation and alters the conformation of DNA in core particles as determined by circular dichroism (Ausio & Van Holde, 1986). It has been found that purified histone acetyltransferases also possess a polyamine acetyltransferase activity (Libby, 1978, 1980), which is probably the activity that acetylates polyamines in a crude nuclear extract (Blankenship & Walle, 1977, 1978). Since acetylation of a polyamine removes one positive charge, it was hypothesized that histone and polyamine acetylation work in concert to facilitate transcription and/or replication of chromatin (Blankenship & Walle, 1978; Morgan et al., 1987). Further experiments have shown that polyamines stabilize and alter the conformation of DNA in the core particle and that acetylation partially reverses these effects (Morgan et al., 1987). These results support the basic hypothesis that transcription and/or replication is facilitated by histone and polyamine acetylation.

Polyamines are organic cations that are actively synthesized by all cells. When cells are stimulated to divide, polyamine levels increase rapidly (Tabor & Tabor, 1976; Janne et al., 1978). Conversely, when cells are deprived of polyamines, cell division is inhibited (Tabor & Tabor, 1984). Thus, polyamines are essential for cell growth and proliferation. Polyamines have a specific effect on expression of the protooncogene c-myc (Celano et al., 1988). Under appropriate conditions in vitro, polyamines bind to and alter the characteristics of polyanions and the proteins that interact with them, including DNA, chromatin, RNA polymerases, RNA, ribosomes, and phospholipids (Tabor & Tabor, 1976, 1984; Braunlin et al., 1982; Porschke, 1984; Sen & Crothers, 1986; Blair, 1985; Morgan et al., 1986, 1987). However, the in vivo relevance of these observations remains obscure. Polyamines are required for cell growth and division and are likely involved in many different primary processes. There may be many steps between the primary effect(s) of polyamines and observed changes such as DNA, RNA, and protein synthesis inhibition (Tabor & Tabor, 1984). Further, due to problems with redistribution, it has been difficult to unambiguously determine the intracellular location of polyamines (Tabor & Tabor, 1984; Pegg & McCann, 1988). All these factors complicate the interpretation of data on polyamine function in vivo.

In eukaryotic cells, the polyamines spermine (+4 charge at neutral pH) and spermidine (+3) are present in variable concentrations on the order of 1 mM, and putrescine (+2) is present in resting cells in concentrations on the order of 10 μM [e.g., McCormick (1978)]. Also, the N^1-acetyl derivatives of spermine and spermidine are present in concentrations on the order of 1 μM (Marchant & Blankenship, 1983; Pegg, 1986; Seiler, 1987). N^8-acetylspermidine is found in urine (Tsuji et al., 1975; Abdel-Monem & Ohno, 1978; Marchant & Blankenship, 1983; Blankenship & Marchant, 1984) and can be detected in tissues in the presence of an inhibitor of polyamine deacetylase (Marchant et al., 1989). In the cytoplasm, the N^1-acetylpolyamines are involved in the metabolism of the polyamines (Pegg, 1986; Seiler, 1987). However, acetylation also occurs in the nucleus, including the formation of N^8-acetylspermidine, the only known fate of which is deacetylation to spermidine (Blankenship & Walle, 1978; Pegg & McCann 1982; Seiler et al., 1981; Pegg, 1986; Seiler, 1987). This reinforces the suggestion that acetylation of polyamines in the nucleus has a functional role in addition to polyamine turnover.

A number of models for polyamine binding to specific sites on DNA have been proposed [e.g., Liquori et al. (1967), Feuerstein et al. (1986), and Zakrewska and Pullman (1986)] as well as a model for completely delocalized binding (Bloomfield & Wilson, 1981). However, although a specific binding site for spermine in a DNA crystal was observed (Drew & Dickerson, 1981), in solution spermine appears to be highly mobile (Wemmer et al., 1985). Several kinds of evidence have been interpreted in terms of specific binding of polyamines to DNA (Basu & Marton, 1987; Basu et al., 1987; Marquet & Houssier, 1988), but the data are indirect and open to multiple interpretations. There is a large body of data consistent with mainly electrostatic binding, with secondary contributions from polyamine structure or DNA base composition (Hirschman et al., 1967; Stevens, 1967; Braunlin et al., 1982; Thomas & Bloomfield, 1984; Thomas et al., 1985; Morgan et al., 1986; Stewart, 1988). The data thus weigh against a single, tightly constrained binding site and support a relatively unconstrained binding site, multiple sites, and/or delocalized binding.

However, experiments on the effects of polyamines, acetylpolyamines, and inorganic cations upon nucleosome core particles yielded results that were not readily explicable by simple electrostatic interactions. In particular, among compounds with a charge of +3, it was found that spermidine was more effective than acetylspermine, which was more effective than hexaamminecobalt at stabilizing core particles against thermal denaturation. Also, in contrast to putrescine and the acetylspermidines (all carrying a charge of +2), magnesium failed to stabilize core particles (Morgan et al., 1987). This was surprising, since magnesium is more effective than putrescine or the acetylspermidines at stabilizing naked DNA (Morgan et al., 1986). Finally, putrescine and the acetylspermidines appear to have slightly greater effect upon the conformation of DNA in the core particle than does magnesium (Morgan et al., 1987). These data suggested that there may be specific or preferred binding sites on the core particle for polyamines, which are not fit as well by the larger acetylpolyamines or the smaller inorganic cations. Equilibrium dialysis studies of spermidine to core particles also suggested the presence of specific binding sites (Dumuis-Kervabon et al., 1986).

The determination of polyamine binding sites has posed an intractable problem for many years. This is due to the fact that polyamines are small molecules and exchange rapidly compared to the time scale of analytical techniques. This was elegantly demonstrated in experiments on *Escherichia coli* nucleoid isolation, where it was found that exogenously added polyamines fractionated identically with cellular polyamines and that added DNA or RNA effectively scavenged cellular polyamines (Rubin, 1977).

We have approached this issue by the use of photoaffinity labeling. In brief, a photoaffinity reagent is allowed to bind noncovalently to the target molecule in a manner similar to the parent compound and then exposed to ultraviolet light. This triggers the formation of a highly reactive species (typically carbene or nitrene), which binds covalently to the target molecule in a short period of time (typically milliseconds) (Bayley, 1983). The site of covalent binding can then be analyzed by conventional techniques. This paper presents the synthesis and characterization of (azidonitrobenzoyl)spermine (ANB-spermine),[1] its use to photoaffinity label nucleosome

[1] Abbreviations: SDS, sodium dodecyl sulfate; CTAB, cetyltrimethylammonium bromide; DTT, dithiothreitol; EDTA, ethylenediaminetetraacetic acid; NH_4OAc, ammonium acetate (pH 7); ANB-spermine, (5-azido-2-nitrobenzoyl)spermine; ANB-NOS, *N*-(5-azido-2-nitrobenzoyl)-*N*-oxysuccinimide; rANB-spermine, (5-amino-2-nitrobenzoyl)spermine; bis, *N*,*N*'-methylenebis(acrylamide); T_m, midpoint of thermal denaturation transition for DNA or nucleosome core particles.

core particles, and the determination of preferred binding sites.

Experimental Procedures

Synthesis of (Azidonitrobenzoyl)spermine. (Azidonitrobenzoyl)spermine (ANB-spermine) was synthesized from *N*-(5-azido-2-nitrobenzoyl)-*N*-oxysuccinimide (ANB-NOS, Pierce Chemical Co.) and spermine (Aldrich, or Research Products International for [^{14}C]spermine). For a ^{14}C-labeled batch, 0.1 mCi of [^{14}C]spermine (90 mCi/mmol in 0.01 M HCl; 1.1 μmol) in 1 mL was added to 2.2 μmol of unlabeled spermine·4HCl in 0.7 mL of water and 0.3 mL of acetonitrile. The pH was adjusted to 10.0 with 0.1 M NaOH. A solution containing 3.3 μmol of ANB-NOS in 0.3 mL of acetonitrile was added and the mixture stirred at room temperature. This solvent system was chosen because of the difficulty of extracting [^{14}C]spermine from the aqueous solvent, in which it is supplied, into organic solvent at high yield. Spermine was used as its own buffer system, which allows the course of the reaction to be followed on a pH meter due to the release of hydrogen ions. The reaction was rapid and almost complete in 1 min, although it was typically allowed to proceed for 5 min, at which time the pH had dropped to 8.2. The pH was adjusted to 7.0 with 0.1 M acetic acid, and NH_4OAc, pH 7, was added to a final concentration of 0.6 M. The mixture was applied to a 1 × 8 cm sulfopropyl-Sephadex column. The column was eluted with 5 mL of 0.6 M NH_4OAc, a gradient of 40 mL of 0.6–1.6 M NH_4OAc, and a wash of 10 mL of 1.6 M NH_4OAc. Fractions were characterized by thin-layer chromatography as described below and liquid scintillation counting. The peak fractions containing the monoderivatized product were pooled, and the NH_4OAc concentration was estimated by conductance and diluted to 0.6 M NH_4OAc. The diluted fractions were reapplied to the column, eluted, and characterized as above. The peak fractions from the second column were pooled, diluted by half with water, and lyophilized. The lyophilized material was redissolved in 8 mL of water. Yield, estimated by absorbance, was 38%.

The above procedure was scaled up to produce a larger, unlabeled batch for nuclear magnetic resonance and other studies. Total quantities of 60 μmol of spermine·4HCl in 7.5 mL of water/acetonitrile, pH 10, and 60 μmol of ANB-NOS in 1.5 mL of acetonitrile were reacted as above. The reaction was divided into two aliquots, and the products were separated on a 1.5 × 17 cm sulfopropyl-Sephadex column, similarly to above. The products were lyophilized, reconstituted in 10 mL of D_2O (Aldrich, 99.8%), and adjusted to pD 3.0 with DCl. This was lyophilized, reconstituted in 1.0 mL of D_2O (Aldrich, 99.96%), and adjusted to pD 5.8 with 0.1 M NaOD. Yield was estimated at 30%.

For the estimation of the extinction coefficient of ANB-spermine, the above synthesis method was modified to eliminate alkaline hydrolysis by using only organic solvents, to ensure that virtually the only product was the monoderivatized form, and to recover the reaction products quantitatively in aqueous solution. To 1 μmol of spermine (free base, 98%) in 50 μL of acetonitrile was added 0.05 μmol of ANB-NOS in 50 mL of acetonitrile. The mixture was allowed to stand for 1 min, and then 860 μL of 10 mM NaCl, 5 mM sodium cacodylate, pH 6.5 with HCl, and 40 μL of 0.1 M HCl were added. The final pH was 6.56. The spectrum from 600 to 220 nm was taken and used to estimate the extinction coefficient.

Characterization of ANB-Spermine. Thin-layer chromatography was performed by a variation of a widely used procedure [e.g., Blankenship and Walle (1977)]. Silica gel (60A) polyester backed plates were developed in 2-propanol/acetic acid/pyridine/H_2O (4:1:1:2). Samples were visualized first with ultraviolet light (366 nm; Ultraviolet Products UVL-56 Blak-Ray) by using the intrinsic fluorescence of the polyester plate. Ultraviolet "dark" spots were marked. Samples were then visualized with ninhydrin. Occasionally, dried plates were autoradiographed by using Kodak XAR-5 film, with one intensifying screen (Du Pont Cronex) for 24 h or as needed.

Quantitative assay for primary amines was performed by using a trinitrobenzenesulfonate procedure modified from Mokrasch (1967). Standard curves were constructed for various polyamines and acetylpolyamines. Typically, at 0.2 mM, spermine or spermidine yielded an $A_{420} = 1.2$ and acetylspermine or acetylspermidine yielded an $A_{420} = 0.7$.

Nuclear magnetic resonance spectroscopy was performed on a Nicolet 360 MHz, Fourier transform instrument. Samples of ANB-spermine at approximately 20 mM (prepared as described above) or spermine at approximately 25 mM in D_2O were scanned, the pD was adjusted upward with NaOD, and the samples were rescanned to generate a titration curve. Spectra were generated from 268 scans, with an initial delay of 4 scans, by using a single 1-μs pulse and 3600-Hz sweep width (10 ppm).

Reverse-phase, ion-pairing high-pressure liquid chromatography was performed as described (Sieler & Knogden, 1980; Marchant & Blankenship, 1983).

Photolysis and Reduction of the Azido Group. Photolysis of ANB-spermine was performed by using either a 366-nm, 750 μW/cm^2 light (Ultraviolet Products UVL-56 Blak-Ray) or a 302-nm, 7000 μW/cm^2 transilluminator (Ultraviolet Products TM-36). The light sources were chosen because they were readily available and reasonably close to the absorbance maximum (320 nm) of ANB-spermine. The light source was placed directly over a small beaker of the solution to be photolyzed.

The azido group of ANB-spermine was reduced to an amino group (product rANB-spermine) with DTT by using a procedure modified from Staros et al. (1978). A 3.0-mL sample of ANB-spermine at 1.2 mM was adjusted to pH 9.0 with NaOH, and 150 μL of 210 mM DTT, pH 9.0 with NaOH, was added. The reaction was allowed to proceed for 30 min at room temperature. The reaction was followed by thin-layer chromatography (above) and changes in the spectrum. A single product was observed, and the reaction was complete by 5 min. The reaction was neutralized and the products separated on a 1.5 × 17 cm sulfopropyl-Sephadex column as above. The pK_a of the aryl amino group of rANB-spermine was estimated by taking the spectra of rANB-spermine diluted into various concentrations of HCl.

Preparation of Nucleosome Core Particles and Thermal Denaturation Studies. Nucleosome core particles were prepared and thermal denaturation was performed as previously described (Morgan et al., 1987). The procedure involves the use of ion-exchange chromatography to strip histone H1 and any endogenous polyamines from the chromatin.

Photoaffinity Labeling. Photoaffinity labeling of core particles with ANB-[^{14}C]spermine was performed by using either a 366- or 302-nm source, as described above. A typical experiment used 6.0 mL of a solution with core particle $A_{260} = 1.0$ (140 μM DNA phosphate) in 1.0 mM NaCl, 0.5 mM sodium cacodylate, pH 6.7 with HCl, plus ANB-[^{14}C]spermine at a charge ratio of 0.1 to 0.5. Charge ratio is defined as the total added cation positive charges divided by total DNA phosphate negative charges. The light source was placed directly over a small beaker containing the stirred solution and

the progress of photolysis monitored by changes in the spectra. Control experiments were also performed that omitted ANB-[^{14}C]spermine. The solution was then dialyzed extensively to remove noncovalently bound ANB-[^{14}C]spermine photoproducts. The most efficient system found for this purpose was dialysis in 3.5-kDa cutoff tubing against 3 changes of 200 volumes of 150 mM NaCl and 5 mM sodium cacodylate, pH 6.5 with HCl, for 24 h each. This was followed by 200 volumes of 10 mM NaCl and 5 mM sodium cacodylate, pH 6.5 with HCl, for 24 h. The solution was concentrated by dialysis against solid poly(ethylene glycol) (20 kDa) to a volume around 1 mL. It was then dialyzed against 200 volumes of 1.0 mM NaCl, 0.5 mM sodium cacodylate, pH 6.7 with HCl, or 20 mM NaCl, 5 mM Tris, and 1 mM Na_2EDTA, pH 8.0 with HCl, for 24 h.

High-Salt Sucrose Gradients. Separation of the components of the photoaffinity labeling reaction was performed on sucrose gradients containing high salt (Godfrey et al., 1980; Eickenbush & Moudrianakis, 1978). Core particles labeled with ANB-[^{14}C]spermine were made 2 M NaCl, 10 mM sodium acetate, and 1 mM Na_2EDTA, pH 5.0, with acetic acid by addition of 2.5× stock. They were centrifuged on 10–27% sucrose gradients in the same buffer at 38000 rpm (260000*g*) in an SW 40Ti rotor for 66 h at 4 °C. The gradients were fractionated, and the A_{276} was monitored. The fractions were dialyzed against 2 mM Na_2EDTA, pH 3.9 with acetic acid, in a 28-well microdialyzer (Bethesda Research Laboratories) for 40 h. Liquid scintillation counting of fractions was performed before and after dialysis. The DNA peak was well resolved, and the amount of radioactivity bound to DNA was determined directly. The protein peak was not completely resolved from the unbound radioactivity. On the assumption that all label in fractions containing histones was covalently bound, an upper limit to the amount of radioactivity bound to protein of 6.6% was obtained. The most likely estimate was that 3.5% of the radioactivity was bound to protein, obtained by assuming that the trailing half of the peak was the same as the leading half, i.e., the peak was symmetrical. A lower limit of 1.3% was obtained by assuming that only the label remaining in histone-containing fractions after dialysis (which removed 90% of the radioactivity in noncovalently bound ANB-[^{14}C]spermine fractions) was covalently bound and that the peak was symmetrical. This is probably an underestimate since variable losses of histones were observed during dialysis. Dialyzed samples were adjusted to the appropriate pH, lyophilized, and run on SDS–protein and SDS–DNA gels (below).

Exonuclease Protection. The locations of covalent binding of ANB-spermine to the DNA of core particles were determined by using an exonuclease protection technique (Gale et al., 1987). The DNA was extracted from photoaffinity-labeled core particles by using phenol/SDS and precipitated with ethanol similarly to the method of Simpson and Whitlock (1976). The DNA was digested with bacterial alkaline phosphatase and 5′ end labeled by using a protocol modified from Bethesda Research Laboratories (undated A). About 25 pmol of 3′ ends of DNA was made 120 mM NaCl and 10 mM Tris, pH 8.0 with HCl, by addition of 5× buffer to give a final volume of 0.1 mL. To this was added 500 units of bacterial alkaline phosphatase, and the reaction was incubated at 65 °C for 60 min. The reaction was extracted with phenol/SDS and precipitated with ethanol. The digestion, extraction, and precipitation were repeated. To the DNA was added 40 μCi of [^{32}P]ATP (Amersham, 3000 Ci/mmol), and the solution was made 10 mM $MgCl_2$, 0.35 μM ATP, 60 mM Tris, and 15 mM 2-mercaptoethanol, pH 7.8, by addition of 5× buffer. To this was added 20 units of T4 polynucleotide kinase, and the reaction was incubated at 37 °C for 30 min. The reaction was phenol/SDS extracted and ethanol precipitated.

The end-labeled DNA was digested by using another protocol modified from Bethesda Research Laboratories (undated B). The DNA was made 10 mM magnesium acetate, 66 mM sodium acetate, 0.5 mM DTT, and 33 mM Tris, pH 7.9 with acetic acid, by addition of 10× buffer. To this was added 40 units of T4 DNA polymerase/exonuclease, and the reaction was incubated at 37 °C. Aliquots were removed at 5, 15, and 30 min, phenol/SDS extracted, and ethanol precipitated. The aliquots were run on urea–DNA gels (below).

DNase I Digestion of Core Particles. End labeling of core particles and DNase I digestion were performed by a protocol modified from Simpson and Whitlock (1976). Thirty units of polynucleotide kinase were added to 96 μL of core particles (A_{260} = 1.2) in 5 mM Tris, 5 mM $MgCl_2$, 5 mM DTT, pH 8.0 with HCl, and 2.8 μM ATP (222 Ci/mmol), and the solution was incubated at 37 °C for 30 min. The reaction was stopped by addition of Na_4EDTA, pH 7.0 with HCl, to 10 mM from 0.1 M stock. The reaction was applied to a 1 × 9 cm Sephadex G-75-40 column and eluted with 20 mM NaCl, 10 mM Tris, and 1 mM Na_2EDTA, pH 8.0 with HCl. Fractions containing core particles (600 μL) were made 10 mM in $MgCl_2$ by addition of 0.1 M stock, 160 μL was removed for the zero time point, and 0.8 μg of DNase I was added. The reaction was incubated at room temperature, and aliquots were removed at 2, 5, and 10 min. Reaction aliquots were extracted with phenol/SDS and ethanol precipitated.

Trypsin Digestion. Photoaffinity-labeled core particles were digested with trypsin by using a protocol modified from Whitlock and Simpson (1977). Typically, 0.3 μg of trypsin (tosylphenylalanine chloromethyl ketone treated, freshly diluted into water from 1 mg/mL stock in 1 mM HCl) was added to 190 μL of core particles at A_{259} = 3.6 (dialyzed into 20 mM NaCl, 5 mM Tris, and 1 mM Na_2EDTA, pH 8.0 with HCl), and the solution was incubated at room temperature. Aliquots of 45 μL were removed at various times (typically 5, 15, 30, and 45 min), and the reaction was stopped by addition of 4× SDS–protein sample buffer (0.32 M Tris, 0.4 M DTT, 8% SDS, 40% glycerol, and 2.5 mg/mL bromophenol blue, pH 6.8 with HCl) and heating to 100 °C for 2 min. Samples were run on an SDS–protein gel as described below.

Particle, SDS–DNA, and SDS–Protein Gels. Particle, SDS–DNA, and SDS–protein gels were used as previously described (Morgan et al., 1987). For fluorography after staining, particle or SDS–DNA gels were shaken in Fluro-Hance (Research Products International) for 1 h; SDS–protein gels were shaken for 2 h in 50% ethanol and then in Fluro-Hance for 1 h. Gels were then dried and exposed to Kodak XAR-5 film at −70 °C with an intensifying screen (Du Pont Cronex) for 1–4 weeks as needed.

CTAB–SDS–Protein Gels. Two-dimensional gels used the cationic detergent CTAB in the first dimension and SDS in the second dimension. The protocol for the CTAB gels was modified from Mocz and Balint (1984) to improve stacking and resolution of core histones. Separating gels contained 15% (w/v) acrylamide, 0.225% (w/v) bis, 62.7 mM KOH, pH 4.56 with acetic acid, and 0.1% CTAB. Stacking gels contained 2.5% (w/v) acrylamide, 0.625% (w/v) bis, 62.7 mM KOH, pH 5.07 with acetic acid, and 0.1% CTAB. The upper reservoir buffer contained 160 mM β-alanine, pH 4.01 with acetic acid, and 0.1% CTAB. The lower reservoir buffer contained

50 mM KOH, pH 5.36 with acetic acid. A 2× sample buffer contained 125 mM KOH, 4% 2-mercaptoethanol, 20% glycerol, 1 mg/mL methyl green, pH 5.07 with acetic acid, and 4% CTAB. Gels were polymerized by using *N,N,N',N'*-tetramethylethylenediamine and riboflavin 5'-phosphate. Samples containing DNA (e.g., core particles) were centrifuged at 13 000 rpm (15000*g*) for 5 min to pellet the DNA, and the supernatant was used for the sample. Samples were heated to 100 °C for 2 min, cooled, and applied to the gel. One-dimensional CTAB gels were stained with Coomassie as described (Mocz & Balint, 1984). For two-dimensional gels, the (unstained) lane of interest was cut out of a CTAB slab gel and rocked with 25 mL of 0.1 M Tris, 0.2 M DTT, 4% SDS, and 0.04 mg/mL bromophenol blue, pH 7.5 with HCl, for $^1/_2$ h. The slice was placed on top of an SDS–protein gel using a chamfered plate and a solution of 1.5% agarose, 0.1% SDS, and 0.125 M Tris, pH 6.8 with HCl, for sealing. The second dimension was run, stained, etc. as described above for SDS–protein gels. Densitometry of fluorographs of these gels was performed by dividing the fluorograph into lanes with the same width as the spectrophotometer light beam, scanning and integrating the bands in each lane, and pooling the integrations for each histone. Scanning was carried out on a correctly exposed fluorograph; Figure 6 shows an overexposed fluorograph for better contrast.

Urea–DNA Gels. Urea–DNA gels were used to examine single-stranded DNA fragments by using a protocol from Maxam and Gilbert (1980), modified to a higher concentration of bis(acrylamide) to suppress sequence-specific variations in mobility (Lutter, 1979; Gale et al., 1987). The gels contained 7.1% (w/v) acrylamide, 0.88% (w/v) bis, and 8 M urea in TBE buffer (90 mM Tris, 90 mM H_3BO_3, and 2.5 mM H_4EDTA, pH 8.1, no adjustment needed). Gels were prerun until the front plate was about 53 °C (72–84 W for 1.5 h). Samples were heated to 100 °C for 2 min, cooled to room temperature, and applied to the gel. Gels were run at about 47 °C (60–66 W), typically until the bromophenol dye was 80% of the distance to the end.

Results

Synthesis and Purification of (Azidonitrobenzoyl)spermine (ANB-Spermine). (Azidonitrobenzoyl)spermine (ANB-spermine) (Figure 1A) was typically synthesized by using equimolar amounts of spermine or [^{14}C]spermine and *N*-(5-azido-2-nitrobenzoyl)-*N*-oxysuccinimide (ANB-NOS; Pierce) in a mixed water/acetonitrile solvent system at pH 10. The reaction products were separated by two passes over a cation-exchange column (sulfopropyl-Sephadex) using an NH_4OAc gradient system. The fractions containing the monoderivatized product (ANB-spermine) were pooled and lyophilized. Yields were 30–40%.

Characterization of ANB-Spermine. ANB-spermine was characterized by thin-layer chromatography, ion-exchange chromatography, reverse-phase, ion-paired high-performance liquid chromatography, spectrophotometry, photoreactivity, reactivity to dithiols, liquid scintillation counting, primary amine assay, and nuclear magnetic resonance. On thin-layer chromatography (see Experimental Procedures), ANB-spermine had an R_f of 0.54, was ultraviolet dark (i.e., contained an aromatic group), ninhydrin positive (i.e., contained a primary amine), and comigrated with the radiolabel as determined by autoradiography. On ion-exchange chromatography (used for purification; see Experimental Procedures) control experiments demonstrated that polyamines and their derivatives eluted mainly as a function of charge; thus, putrescine (+2) eluted near 0.70 M, spermidine (+3) near 0.95 M, and spermine (+4) near 1.12 M NH_4OAc. ANB-spermine eluted near spermidine, indicating a +3 charge. It was somewhat surprising to us that only one monoderivatized reaction product was observed. To search explicitly for minor products, ANB-spermine was run on a reverse-phase, ion-pairing high-performance liquid chromatography system that is commonly used to resolve polyamines and acetylpolyamines (Seiler & Knogden, 1980; Marchant & Blankenship, 1983). It was found that only one peak of ANB-spermine was observed, which eluted late in the gradient, and that detection by fluorescence (*o*-phthaldehyde) was suppressed by 97%. Also, small amounts (less than 1%) of spermidine, which was a minor contaminant in the reactant spermine, and ammonia, which was left from lyophilization of the column eluent, were detected.

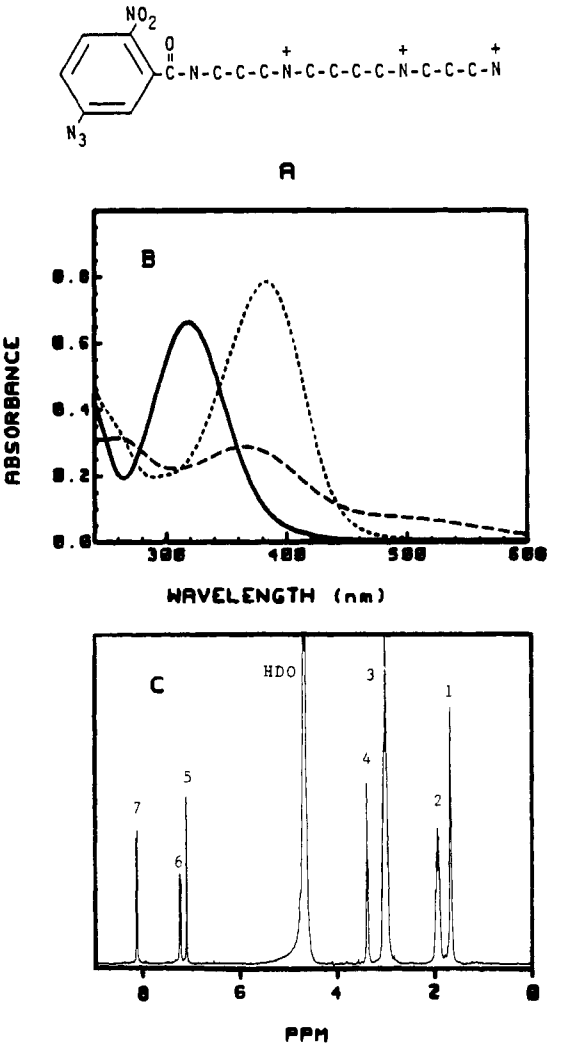

FIGURE 1: (Azidonitrobenzoyl)spermine (ANB-spermine). (A) Structure. (B) Absorption spectra. ANB-spermine (—); rANB-spermine (ANB-spermine reduced with DTT) (---); ANB-spermine photolyzed with 366-nm light (– –). (C) Nuclear magnetic resonance spectrum. Peak group numbers correspond to text and Table I. HDO peak also indicated.

The spectrum of ANB-spermine had an absorbance maximum at 320 nm (Figure 1B). The E_{320} was estimated as 1.12 × 10^{+4} M^{-1} cm^{-1} (see Experimental Procedures). By comparison, the parent compound, ANB-NOS, has an E_{320} of 1.04 × 10^{+4} M^{-1} cm^{-1}. Photolysis produced a significant change in the absorbance spectrum, characterized by the loss of absorbance at 320 nm and the development of new peaks around 260 and 365 nm (Figure 1B). Using a 0.5 mM solution, $t_{1/2}$ values of 40 and 15 s were observed with a 366-nm, 750

Table I: Nuclear Magnetic Resonance Spectra of ANB-Spermine and Spermine

compound	peak (Figure 1C)	integrate (H)	shift[a] (ppm)	pD shift[b] (ppm)	assignment
ANB-spermine	1	4	1.66	−0.25	C6,7
	2[c]	4	1.94	−0.24–0.41	C2,11
	3	10	3.01	−0.47	C3,5,8,10,12
	4	2	3.38	−0.07	C1
	5	1	7.10	−0.02	benzoyl
	6	1	7.23	0	benzoyl
	7	1	8.13	−0.01	benzoyl
spermine	1	4	1.65	−0.27	C6,7
	2	4	1.95	−0.44	C2,11
	3	12	2.98	−0.48	C1,3,5,8,10,12

[a] Shift(ppm) is the chemical shift of the average of each group of peaks at pD 5.80 for ANB-spermine and at pD 5.50 for spermine (both are completely charged at these pD values). [b] pD shift (ppm) is the change in chemical shift for a change in pD from 5.80 to 11.35 (ANB-spermine) or from 5.50 to 11.41 (spermine). [c] Peak group 2 for ANB-spermine splits into two groups around pD 9.

$\mu W/cm^2$ and a 302-nm, 7000 $\mu W/cm^2$ light source, respectively. Photolysis produced a number of products that could be resolved on thin-layer and ion-exchange chromatography, including a putative intramolecular circularization (+2 charge), two solvent and/or rearrangement products (+3 charge), and a dimerization (greater than +4 charge). The azido group of ANB-spermine could also be rapidly reduced to an amino group (rANB-spermine) with DTT at basic pH (Staros et al., 1978). The rANB-spermine has a characteristic absorbance maximum at 383 nm (Figure 1B) and an E_{383} of $1.3 \times 10^{+4}$ M^{-1} cm^{-1}. The pK_a of the aryl amino group was estimated to be 0.0 by monitoring the change in spectrum with pH, which is similar to the pK_a for *p*-nitroaniline of 1.0.

The structure of ANB-spermine was initially determined chemically from measurements of the concentrations of core [^{14}C]spermine molecules (by liquid scintillation counting), primary amines (by trinitrobenzenesulfonate assay), and azidonitrobenzoyl groups (by absorbance). The ratios of primary amine and azidonitrobenzoyl groups to core spermine were 0.98 and 1.09, respectively, with errors in the combined assays of 5–10%. The results were clearly different from the only other unique possibilities, 0 or 2, and indicate the structure shown in Figure 1A. However, the results do not rule out the possibility of other minor (5–10%) species being present.

Independent confirmation of thestructure was obtained by nuclear magnetic resonance spectroscopy of ANB-spermine (Figure 1C) and spermine. Spectra were taken at various pDs, and the chemical shifts at low and high pDs were compared (Table I). ANB-spermine had seven peaks or groups of peaks, compared to three for spermine. Three of the unique ANB-spermine peaks (5, 6, and 7) are shifted far downfield (7.10–8.13 ppm), are not perturbed by titration, and integrate to 1 H each. These clearly belong to the hydrogens on the azidonitrobenzoyl group. The fourth unique ANB-spermine peak (4) is somewhat downfield from the spermine peaks (3.38 ppm at pD 5.8), is affected slightly by titration, and integrates to 2 H. These characteristics are similar to those of a methylene peak that is adjacent to the amide groups in acetylspermidines (Dr. Mike Minch, University of the Pacific, Stockton, CA, personal communication). The fact that this peak integrates to 2 H, not 4 H, indicates unequivocally that the major molecular species is monoderivatized, not diderivatized, and that this occurred at a primary, not a secondary, amine. It is still possible, though, that a small amount of another molecular species was present (less than 5–10%).

Noncovalent Binding of ANB-Spermine to Core Particles. To test the noncovalent binding of ANB-spermine to core particles, thermal denaturation was performed (Figure 2A).

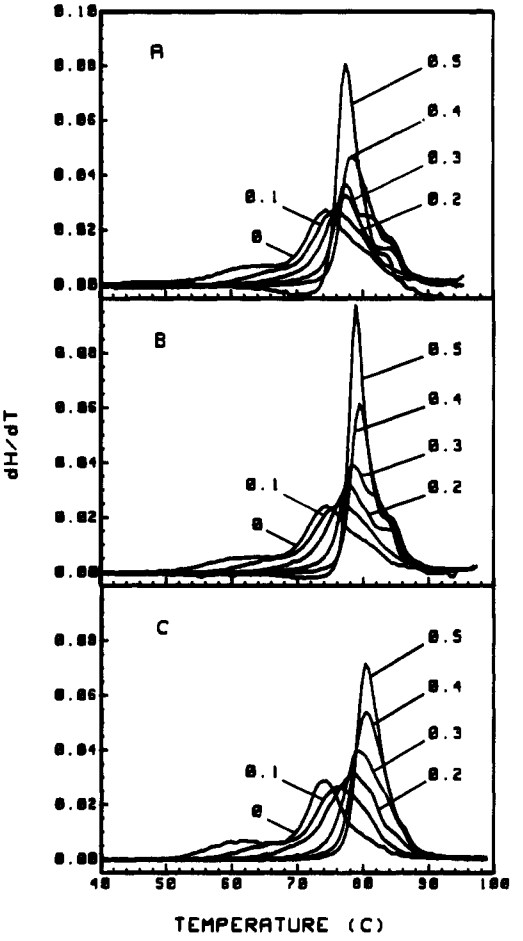

FIGURE 2: Thermal denaturation profiles of core particles with added (A) ANB-spermine, (B) rANB-spermine (ANB-spermine reduced with DTT), and (C) acetylspermine. Core particle A_{259} = 0.645 in 1 mM NaCl and 0.5 mM sodium cacodylate, pH 6.7 with HCl. Polyamines were added at charge ratios indicated (0, 0.1, etc.) (charge ratio defined as total added polyamine positive charge/total DNA phosphate negative charge).

Comparison with the thermal denaturation profiles of other polyamines with the same charge [acetylspermine, Figure 2C; spermidine, see Figure 2B of Morgan et al. (1987)] shows that the effects are qualitatively similar. Particularly notable are the suppression of premelt, substantial increase in melting temperature (T_m) of the premelt and main transition, and sharpening of the main transition. The response was qualitatively different from that observed with the parent compound spermine [Figure 2A of Morgan et al. (1987)], in the lack of precipitation at charge ratio 0.5 and lack of hypersharpening of the main transition. One problem with these studies is that the aryl azido group of ANB-spermine could be photolyzed by the incident 259-nm light in the spectrophotometer. Spectra from before and after thermal denaturation indicate that 10–15% was, in fact, photolyzed. This relatively low level of photolysis was probably due to the incident light being of low intensity and far from the absorbance maximum of ANB-spermine (320 nm). Nonetheless, the photolysis products appear to include compounds significantly different from the original compound, as discussed above, and probably a small amount of covalent binding as well. To circumvent these problems, thermal denaturation was performed on rANB-spermine, in which the aryl azido group had been reduced to an aryl amino group by using DTT. Since the aryl amino group was found to have a pK_a of 0.0 (i.e., was not charged under these experimental conditions) and is of comparable size to the azido group, this compound is a good model for

ANB-spermine in thermal denaturation experiments. It was found to behave qualitatively similarly to ANB-spermine, acetylspermine, and spermidine (Figure 2B).

The melting profiles were quantitated by using Gaussian fitting as described in Morgan et al. (1987). At this level of analysis, both similarities and differences between ANB-spermine, rANB-spermine, and the naturally occurring polyamines emerged. First, it was found that the increase in T_m was greatest for ANB-spermine and rANB-spermine from charge ratio (defined as total added polyamine positive charge/total DNA phosphate negative charge) 0 to 0.3 and that a plateau occurred at higher concentrations. This indicates a similar saturation effect to that observed with acetylspermine and spermidine. However, the T_ms at charge ratio 0.4 (near saturation) were somewhat lower for ANB-spermine and rANB-spermine. Indeed, an ordering was observed, with the T_ms for spermidine > acetylspermine > rANB-spermine > ANB-spermine in steps of 0.3–0.9 °C. Thus, the presence of bulky side groups reduces the stabilization of core particles by polyamines, but does not qualitatively alter it. It is likely that this is a reflection of lowered binding strength.

Photoaffinity Labeling of Core Particles with ANB-Spermine. Photoaffinity labeling was performed by mixing core particles with ANB-[^{14}C]spermine at charge ratios 0–0.5 and irradiation with either a 366- or a 302-nm light source as above. Results with the two light sources were similar, except that putative pyrimidine dimers were formed in the core particle DNA when the 302-nm source was used (see below). The time course of photolysis was followed by observing changes in the spectra, similar to those in Figure 1B. It was observed that the 366-nm source yielded a $t_{1/2}$ of 15–20 s and was allowed to proceed for 4 min. The 302-nm source yielded a $t_{1/2}$ around 12 s and was allowed to proceed for 1.5 min. Noncovalently bound ANB-[^{14}C]spermine photoproducts were removed by dialysis. It was found that higher concentrations of salt and longer periods of dialysis aided removal. The most efficient removal was with 155 mM Na^+. This was the highest salt concentration examined, due to reports that dissociation of the DNA is favored at higher salt concentrations and more dilute core particle concentrations (Ausio et al., 1984; Cotton & Hamkalo, 1981). During the last change of 155 mM Na^+ buffer, only 1–1.5% of the input ANB-[^{14}C]spermine came off, and none came off in subsequent low-salt dialyses and concentration. Typically, 27–32% of the input ANB-[^{14}C]-spermine remained associated with the core particles after dialysis and concentration.

The ANB-[^{14}C]spermine photoaffinity-labeled core particles recovered from dialysis were characterized on particle, SDS–DNA, and SDS–protein gels. On particle gels, where the core particle migrates as a structure distinct from DNA, it was observed that the core particles were intact, and the ANB-[^{14}C]spermine label comigrated with the particles (Morgan, 1988). However, this label could have been noncovalently bound, since the low ionic strength conditions would not dissociate noncovalently bound polyamines. It was also observed that the mobility of the core particles decreased as increasing amounts of ANB-[^{14}C]spermine were bound.

On SDS–DNA gels, it was observed that the DNA was intact and that (at least some) of the ANB-[^{14}C]spermine comigrated with the DNA (Morgan, 1988). Control experiments indicated that noncovalently bound, photolyzed ANB-[^{14}C]spermine did not comigrate with the DNA in these gels. Again, it was observed that the mobility of the DNA decreased as increasing amounts of ANB-[^{14}C]spermine were bound. This could be due either to the loss of net charge or to bending of the DNA resulting from ANB-[^{14}C]spermine binding. In support of the latter hypothesis, no alteration of mobility was observed when the same DNA was run on urea–DNA gels, where the DNA is single stranded (see below). Energy minimization modeling of spermine bound to DNA yields a bent DNA molecule (Feuerstein et al., 1986), and bent DNA displays reduced electrophoretic mobility (Trifonov, 1984).

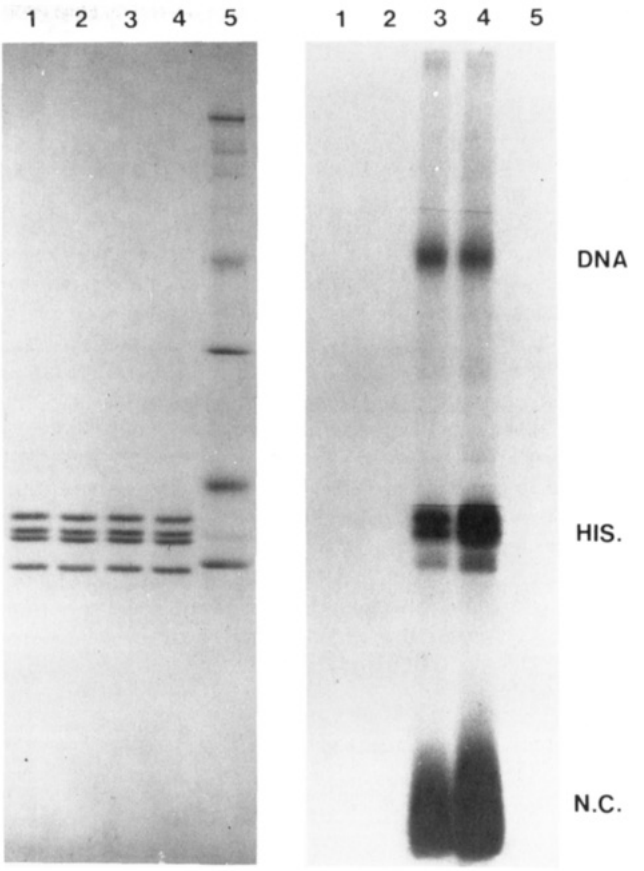

FIGURE 3: SDS–protein gel of core particles. (Left) Coomassie stain; (right) fluorograph. (Lane 1) Core particles; (lane 2) core particles exposed to 302-nm light. (Lanes 3 and 4) core particles photoaffinity labeled with ANB-[^{14}C]spermine by using 302-nm light, (lane 3) charge ratio 0.2, (lane 4) charge ratio 0.4; (lane 5) Bio-Rad low molecular weight standards. Positions of denatured DNA (DNA), histones (HIS.), and noncovalently bound ANB-[^{14}C]spermine photoproducts (N.C.) are indicated.

On SDS–protein gels, it was observed that the histones were intact and that some of the ANB-[^{14}C]spermine label comigrated with the histones (Figure 3). Fluorographs and Coomassie stain were aligned by using a radiolabeled marker pen; the label trailed slightly behind the Coomassie-stained bands, and it appeared that histones H3 and H2B were more highly labeled. These gels were particularly instructive, as the DNA, which had been denatured by heating the sample to 100 °C, has a mobility equivalent to that of a 52-kDa protein. Again, some label comigrated with the DNA. Control experiments indicated that noncovalently bound, photolyzed ANB-[^{14}C]spermine migrated near the dye front, likely due to formation of complexes with SDS, but did not comigrate with either the DNA or histones. The amount of noncovalently bound ANB-[^{14}C]spermine photoproducts appeared to be greater than that comigrating with either the DNA or histones. Control experiments demonstrated that this was due neither to the presence of DTT in the sample buffer nor to heating the sample. Qualitatively, it thus appears from these gels that there was covalent binding to the DNA and histones, but that

a significant amount of noncovalently bound ANB-[^{14}C]-spermine photoproducts remained. However, these results were not regarded as quantitative, since it seemed likely that there was some loss of the noncovalently bound polyamines during staining and fluorography.

To quantitate the amount of covalent binding to DNA and histones, we sought a method that would both separate and allow quantitative recovery of all the components. Since DNA dissociates from core histones in 2 M NaCl (Godfrey et al., 1980; Eickenbush & Moudrianakis, 1978), we reasoned that the smaller, noncovalently bound ANB-[^{14}C]spermine photoproducts would also. Sucrose gradients containing 2 M NaCl at pH 5 were found to give a clean spearation of DNA and a partial separation of histones from noncovalently bound ANB-[^{14}C]spermine products. All of the label loaded as sample was recovered within experimental error (±3%). By use of core particles that had been photoaffinity labeled at charge ratio 0.3, it was found that 3.0% of the input ANB-[^{14}C]spermine was covalently bound to the DNA and approximately 3.5%, within a factor of 2, was bound to histones (see Experimental Procedures). Significantly, the pattern of labeling observed for the separated components, when resolved on SDS–DNA and SDS–protein gels, very closely resembled the pattern observed for the unseparated components on the same gels.

As noted above, 27–32% of the input ANB-[^{14}C]spermine remained associated with the core particles following extensive dialysis. Since the high-salt sucrose gradients indicated that only 3% of the input was covalently bound to DNA, and a similar amount to histones, it appears that the majority remaining after dialysis was noncovalently bound. This is consistent with the SDS–protein gel data. The noncovalently bound compounds may have been formed during photoaffinity labeling and resisted dialysis (as might be expected for higher multimers of ANB-spermine) or may have been formed subsequently by hydrolysis of labile covalent bonds.

Location of Covalent Binding Sites on DNA. An exonuclease protection technique was used to determine the locations of covalent binding of ANB-spermine to DNA in core particles. Briefly, core particles were photoaffinity labeled with ANB-spermine, and the DNA was extracted, digested with bacterial alkaline phosphatase (to remove 3′ phosphates), 5′ end labeled with ^{32}P, and digested for varying times with T4 DNA polymerase–exonuclease. The latter enzyme possesses a 3′–5′ exonuclease that stops at pyrimidine dimers (Doetsch et al., 1985; Gale et al., 1987). Also, it will not digest DNA with a 3′ phosphate, as left by micrococcal nuclease preparation of core particles. It seemed plausible that it might also stop or pause at covalently bound ANB-spermine; this was found to be the case. A time course of the exonuclease digestion of DNA from control core particles irradiated with 366-nm light showed that the DNA was digested to short oligonucleotides with no pauses (Figure 4). A small amount (less than 0.15%) of the original length DNA remained, due to incomplete removal of 3′ phosphate. In contrast, the time course of digestion of DNA from core particles photoaffinity labeled with ANB-spermine by using 366-nm light showed that resistant bands were formed at six positions, and there was a 4–5-fold increase in the amount of resistant original length DNA (Figure 4). Thus, there is actually a seventh position at the 3′ terminus. Whether there was an eighth position near the 5′ terminus could not be determined with this system. These bands were superimposed upon an otherwise featureless background of resistant DNA. It was observed that the intensity of the resistant bands decreased with increasing digestion time, which indicates that the exonuclease pauses, but does not stop completely, at the bound ANB-spermine. Also, by use of DNA from core particles labeled with increasing amounts of ANB-spermine, it was found that the intensity of the resistant bands increased as the amount of labeling increased. Finally, when naked DNA (which had been extracted from core particles) was labeled, all bases were equally resistant to digestion by the exonuclease, i.e., there were no preferred binding sites.

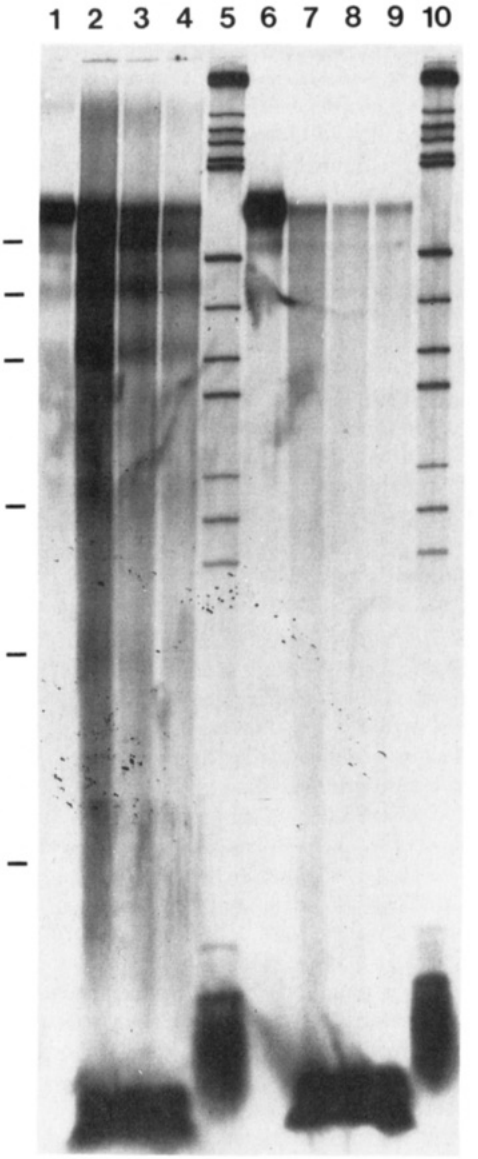

FIGURE 4: Time course of digestion with T4 DNA polymerase–exonuclease. An autoradiograph of a urea–DNA gel is shown. (Lanes 1–4) DNA from core particles photoaffinity labeled with ANB-spermine at charge ratio 0.3 by using 366-nm light. Locations of resistant bands are indicated (—). (Lanes 6–9) DNA from control core particles exposed to 366-nm light. (Lanes 1 and 6) 0′; (lanes 2 and 7) 5′; (lanes 3 and 8) 15′; (lanes 4 and 9) 30′. Note that lanes 1 and 6 were loaded with $^1/_{50}$ the volumes of lanes 2–4 and 7–9. (Lanes 5 and 10) Molecular weight standards from pBR322/*Hae*III.

The length of the resistant bands was determined by comparison to DNase I digests of ^{32}P-labeled core particles (Simpson & Whitlock, 1976; Lutter, 1979; Prunell et al., 1979). It was found that the resistant bands were centered 15, 36, 56, 86, 109, and 130 bases from the 3′ end, on the basis of the DNase I assignments of Lutter (1979) (Figure 5). The resistant bands were 3–6 bases in width, which is slightly greater than the original DNA width or that of the DNase I bands. Relative to the center of the DNA molecule (around

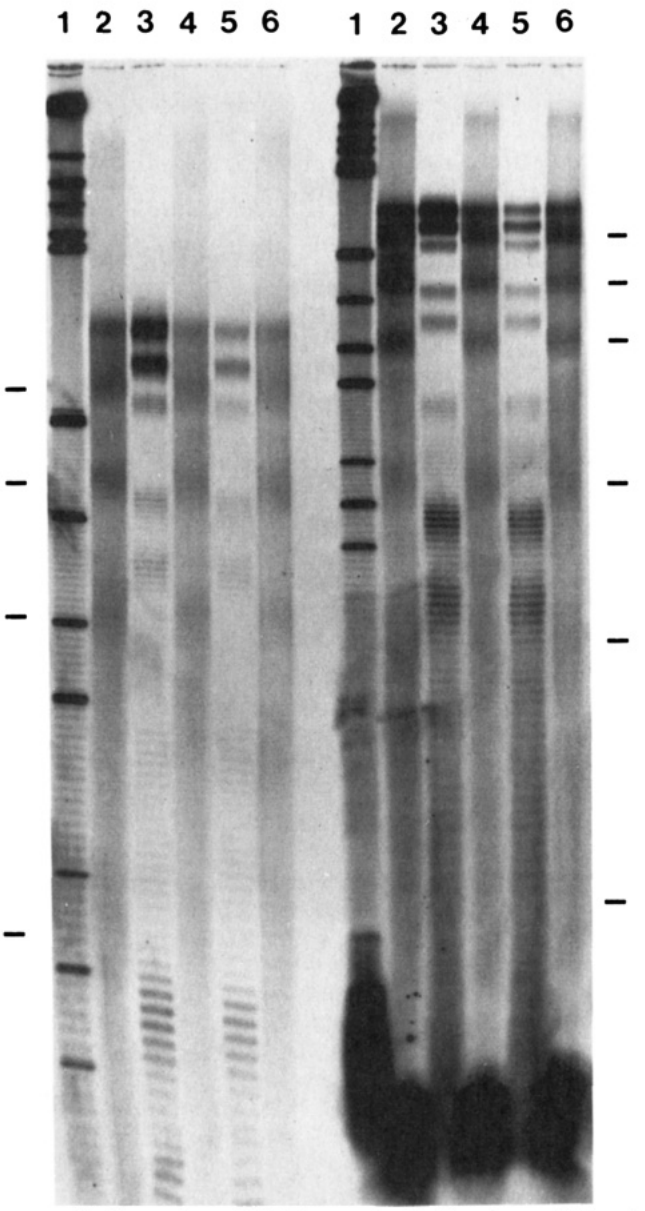

FIGURE 5: Comparison of ANB-spermine binding sites to DNase I nicking sites. An autoradiograph of a urea–DNA gel is shown. (Lanes 2, 4, and 6) T4 DNA polymerase–exonuclease digest of DNA from core particles photoaffinity labeled with ANB-spermine at charge ratio 0.3 by using 366-nm light. (Lane 2) 5′; (lane 4) 15′; (lane 6) 30′. Locations of resistant bands are indicated (—). (Lanes 3 and 5) DNase I digest of core particles. (Lane 3) 5′; (lane 5) 10′. (Lane 1) Molecular weight standards from pBR322/*Hae*III. The left half of the gel was run for a longer time than the right half.

73 bases), the bands are at −58, −37, −17, +13, +36, and +57 bases. Thus, the bands are nearly symmetrical about the center of the DNA molecule, and, considering their width, the bands on one strand of the DNA helix overlap those on the other, which indicates that both strands of the helix at each site are labeled. The resistant bands are spaced 21, 20, 30, 23, and 21 bases apart. Thus, the positions do not follow a simple 10-bp repeat. Surprisingly, it was found that the internal positions did not overlap the DNase I nicking sites: rather, they were offset by 3–5 bases (Figure 5).

One serious potential source of artifact in these experiments was the possibility that single-stranded DNA molecules with covalently attached ANB-spermine might have an altered electrophoretic mobility on urea–DNA gels, as was observed for double-stranded DNA on SDS–DNA gels (above). This was addressed by comparing DNA from core particles to DNA

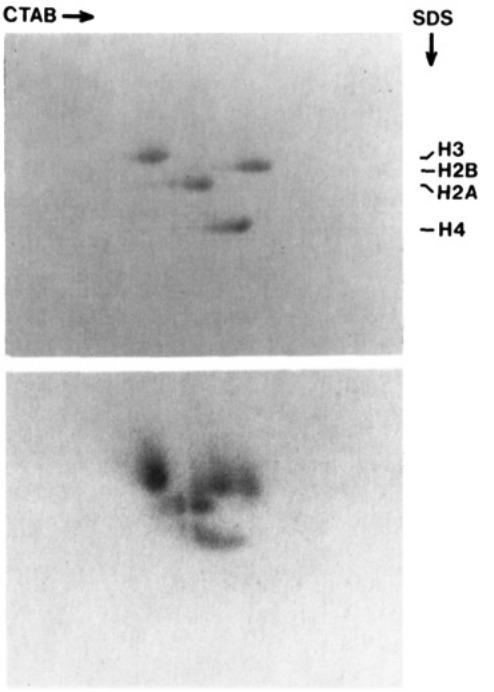

FIGURE 6: Two-dimensional gel electrophoresis of core particles photoaffinity labeled with ANB-[^{14}C]spermine at charge ratio 0.3 by using 366-nm light. First dimension CTAB; second dimension SDS. (Upper panel) Coomassie stain; (lower panel) fluorograph.

from core particles with the 3′ phosphate removed, and DNA from photoaffinity-labeled core particles with the 3′ phosphate removed. It was found that there was no detectable change in mobility due to dephosphorylation. It was found that labeling at roughly one ANB-spermine per two single-stranded DNA molecules resulted in a loss of resolution of the individual bands, but no overall change in mobility. Hence, binding of ANB-spermine results in an alteration of less than 0.5 base in apparent mobility of DNA on urea–DNA gels.

As mentioned above, similar experiments were performed by using core particles irradiated or photoaffinity labeled with 302-nm light. Control core particles irradiated with 302-nm light developed a set of resistant bands with mobilities close to those of DNase I digestion fragments, unlike those irradiated with 366-nm light that showed no resistant bands. Irradiation of core particles with some wavelengths of ultraviolet light induces the formation of pyrimidine dimers with a similar periodicity to DNase I fragments (Gale et al., 1987). The DNA from core particles photoaffinity labeled with 302-nm light developed a set of resistant bands that appeared to be a combination of putative pyrimidine dimers and ANB-spermine binding sites.

Locations of Covalent Binding Sites on Histones. As indicated above, photoaffinity labeling of core particles with ANB-spermine results in appreciable covalent binding to histones. However, on SDS–protein gels, the closeness of the histone bands and the trailing of the ANB-[^{14}C]spermine label made identification and quantitation ambiguous. Also, there was concern that the noncovalently bound ANB-[^{14}C]spermine photoproducts might bind to SDS–histone complexes, yielding misleading results. To help resolve these questions, a two-dimensional gel system, employing the cationic detergent CTAB in the first dimension and the anionic detergent SDS in the second dimension, was used. This results in improved separation mainly because histone H2B runs ahead of the other core histones in the CTAB dimension. It was found that the ANB-[^{14}C]spermine label comigrated with the histones, al-

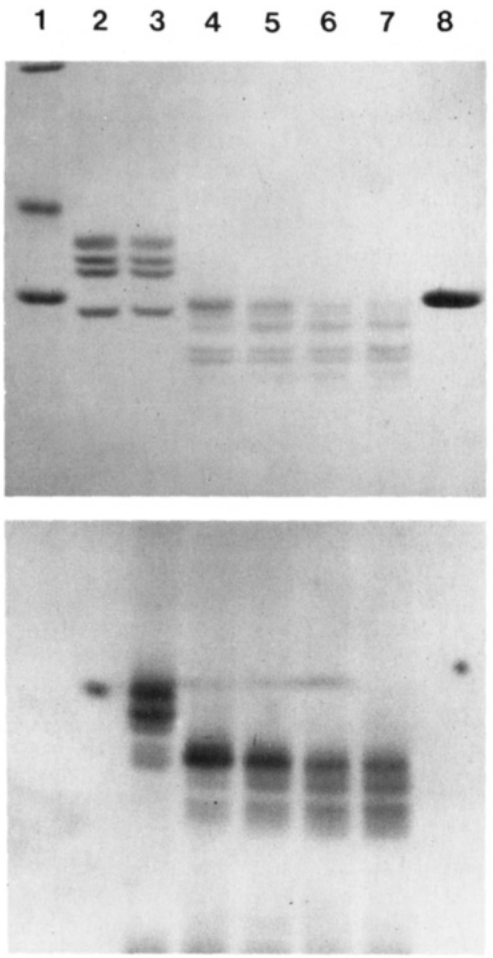

FIGURE 7: Trypsin digestion of core particles photoaffinity labeled with ANB-[^{14}C]spermine at charge ratio 0.3 by using 366-nm light. An SDS–protein gel is shown. (Upper panel) Coomassie stain; (lower panel) fluorograph. (Lane 1) Bio-Rad low molecular weight standards. (Lane 2) Core particles. (Lanes 3–7) Trypsin digest of photoaffinity labeled core particles. (Lane 3) 0′; (lane 4) 5′; (lane 5) 15′; (lane 6) 30′; (lane 7) 45′. (Lane 8) Lysozyme standard.

though it trailed in both dimensions (Figure 6). Densitometry of the fluorograph showed that the label was distributed H3 = H2B > H2A > H4 (30%:32%:21%:17%). Since there is no reason to believe that the noncovalent ANB-[^{14}C]spermine photoproducts would complex with the CTAB-histone complexes, this is unambiguous evidence that the core histones are labeled and that histones H3 and H2B are the favored sites.

It was also of interest to know which regions of the histones were labeled. The core histones have central globular regions and random-coil N-terminal tails. The N-terminal tails can be removed by digestion of the core particle with trypsin [reviewed in Bohm and Crane-Robinson (1984)]. When trypsin digestion was used to probe core particles photoaffinity labeled with ANB-[^{14}C]spermine, it was found that the majority of the label (73–80% by densitometry) remained associated with the trypsin-resistant globular regions (Figure 7). Thus, the core histones are labeled predominantly in the central globular regions.

Discussion

The above results show that the polyamine photoaffinity reagent (azidonitrobenzoyl)spermine (ANB-spermine) (Figure 1A) has been synthesized and purified. This reagent can be produced in either ^{14}C-labeled or unlabeled form. On a noncovalent level it interacts with nucleosome core particles similarly to naturally occurring polyamines, as determined by thermal denaturation. However, the bulky ANB group appears to interfere to a small extent with binding, in common with the uncharged regions of naturally occurring acetylpolyamines. Unfortunately, the classical photoaffinity control experiment, involving competition of the photoaffinity reagent with the parent compound, cannot be performed in this system, because excess polyamines precipitate core particles (Dumuis-Kervabon et al., 1986).

When ANB-spermine was used to photoaffinity label nucleosome core particles, covalent binding occurred at about 3% efficiency for the DNA and a similar (within a factor of 2) efficiency for the histones. This is qualitatively similar to the results of Nielsen (1985), who found that an (azidoaryl)bis(acridinyl)spermidine probe of chromatin (which binds by intercalation to DNA) yielded about 1% labeling efficiency to DNA and 5–10% to protein. Exonuclease protection experiments showed that there were seven preferred sites of ANB-spermine labeling of the DNA: at the 3′ end, and at positions 15, 36, 56, 86, 109, and 130 bases from the 3′ end. A possible position near the 5′ end could not be determined with this method. Also, there was a featureless background of resistant DNA (compared to controls), which could indicate nonspecific binding and/or be due to molecules just released from a pause in digestion. The position at the 3′ end may be due to greater accessibility of the bases at the end of the molecule to chemical reaction with the nitrene, i.e., be an end effect which would not be present in longer chromatin. The resistant bands were 3–6 bases wide, which is wider than either the initial DNA distribution or the DNase I bands. The positions were roughly symmetrical about the center of the DNA molecule (about 73 bases) and, considering the width of the bands, overlapped from one strand of the DNA helix to the other, which indicates that both strands of the helix were labeled at each site. Surprisingly, comparison to DNase I nicking sites showed that there was no overlap between the two (Figures 5 and 8). Since DNase I is a relatively large molecule, it nicks DNA at sites on the outside of the core particle (Lutter, 1979; Prunell et al., 1979). The conclusion which must be drawn from this is that the preferred sites of ANB-spermine labeling are in some sense "inside" the core particle. This conclusion was reinforced by trypsin digestion studies, which showed that the labeling sites on histones were mainly in the central, globular regions (73–80%), rather than on the tails which appear to be on the outside of the particle (Bohm & Crane-Robinson, 1984).

In the nucleosome core particle, the DNA is wrapped in a supercoil of about 1.8 turns around the histone core (Richmond et al., 1984; Morse & Simpson, 1988). Figure 8 shows the approximate locations of the ANB-spermine binding sites mapped onto the DNA as it is wrapped around the protein core of the nucleosome core particle (Richmond et al., 1984). The diagram suggests that the sites occur where the minor groove faces in toward the protein core but does not indicate whether ANB-spermine binds across either groove of the DNA. When the preferred labeling sites are mapped on the DNA positions on an intact core particle, all of the sites are found to be in regions of the particle where one turn of the DNA supercoil is closely apposed to the adjacent turn of the supercoil. Indeed, there is a conspicuous gap of preferred binding sites where there is only a single turn of the supercoil (positions between the labels 0 and 1 in Figure 8B). The simplest interpretation of these observations is that the preferred ANB-spermine binding sites lie between the two turns of the DNA supercoil on the core particle, not on the outside surface. This is plausible in that the regions of highest negative

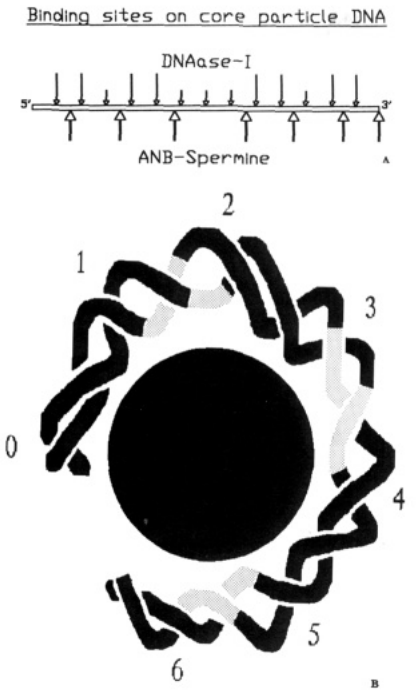

FIGURE 8: Diagram of preferred ANB-spermine binding sites. (A) One strand of the core particle DNA is represented on a linear map. The upper, small, arrows represent the sites of cleavage by DNase I; long shafts on the arrows indicate strong cleavage sites. The lower arrows, pointing upward, indicate the positions of ANB-spermine binding and show the offset from DNase I cuts. (B) An approximate representation of the path of the DNA around half of the core particle is shown [on the basis of a computer scan of half of the stereo pair presented in Richmond et al. (1984)]. The positions labeled 0–6 are the positions where the minor groove faces out; position 0 is at the center of the core particle DNA; the diad axis runs horizontally through position 0. There is approximately half turn of disordered DNA not shown beyond the label 6 (Richmond et al., 1984). Crosshatching along the DNA indicates the approximate sites of binding of ANB-spermine. The sites of ANB-spermine binding are located approximately half turn of the double helix from the positions where the minor groove points out. The positions are approximate because we were unable to make precise measurements in three dimensions from the published data on the DNA path. The direction of the strand was deduced from the handedness of the double helix.

charge would be where the DNA phosphates from the two turns are most closely apposed. This would enhance ANB-spermine binding in these regions and facilitate other, weaker interactions such as hydrogen bonding. Alternatively, the kink in the DNA near the center of the nucleosome (Richmond et al., 1984; Morse & Simpson, 1988) could inhibit the formation of a polyamine binding site. The observed binding sites are probably large enough to accommodate more than one ANB-spermine molecule (perhaps three to four each). Since ANB-spermine binds noncovalently to core particles similarly to other polyamines of charge +3, it is likely that the sites of photoaffinity labeling represent general preferred polyamine binding sites. The X-ray data (Richmond et al., 1984) show electron density close to the DNA in the regions of the ANB-spermine binding sites, which is consistent with the presence of spermine at these sites in the crystals.

Acetylation of polyamines reduces their ability to stabilize and alter the conformation of DNA in core particles (Morgan et al., 1987). The effects of acetylation were similar in magnitude and direction to the effects of acetylation of the core histones (Ausio & Van Holde, 1986). Since histone acetyltransferases also acetylate polyamines (Libby, 1978, 1980), it follows that these enzymes would not only be able to modify the characteristics of the core particle by reaching the exposed histone tails, but would, by virtue of polyamine exchange, be able to reach inside the particle as well, rather as a key unlocks a door. It seems plausible that the combination of these two events would be useful in relaxing or opening up chromatin to facilitate transcription and/or replication.

These experiments raise the question of whether polyamines actually bind to chromatin in vivo. Recent experiments have shown that polyamine derivatives can substitute for spermine or spermidine in polyamine-starved cells (Nagarajan et al., 1988), and preliminary results from this laboratory indicate that some polyamine photoaffinity analogues are taken up by yeast cells (E. Clark and T. Castro, unpublished results). Thus, the development of photoaffinity methods for polyamines, as described above, may offer an opportunity to study polyamine localization in vivo.

ACKNOWLEDGMENTS

We are deeply indebted to Dr. Jim Blankenship for his encouragement, advice, and insight on this project. We thank Dr. Mike Minch and Dr. Claude Meares for helpful discussions, Dr. Mark Knudsen (nuclear magnetic resonance) and Dr. Pamela Marchant (HPLC) for technical assistance, and Christopher Houser for preparing Figure 8B.

Registry No. ANB-NOS, 60117-35-3; ANB-spermine, 120547-02-6; rANB-spermine, 120547-03-7; spermine, 71-44-3; acetylspermine, 25593-72-0.

REFERENCES

Abdel-Monem, M. M., & Ohno, K. (1978) *J. Pharmaceut. Sci. 61*, 161–167.

Allegra, P., Sterner, R., Clayton, D. F., & Allfrey, V. G. (1987) *J. Mol. Biol. 196*, 379–388.

Allfrey, V. G. (1977) in *Chromatin and Chromosome Structure* (Li, H. J., & Eckhardt, R. A., Eds.) pp 167–191, Academic Press, New York.

Allfrey, V. G., Faulkener, R. M., & Mirsky, A. E. (1964) *Proc. Natl. Acad. Sci. U.S.A. 51*, 786–794.

Annunziato, A. T., & Seale, R. L. (1983) *Mol. Cell. Biochem. 55*, 99–112.

Ausio, J., & Van Holde, K. E. (1986) *Biochemistry 25*, 1421–1428.

Ausio, J., Seger, D., & Eisenberg, H. (1984) *J. Mol. Biol. 176*, 77–104.

Basu, H. S., & Marton, L. J. (1987) *Biochem. J. 244*, 243–246.

Basu, H. S., Shafer, R. H., & Marton, L. J. (1987) *Nucleic Acids Res. 15*, 5873–5886.

Bayley, H. (1983) Photogenerated Reagents in Biochemistry and Molecular Biology, *Lab. Tech. Biochem. Mol. Biol. 12.*

Bethesda Research Laboratories (undated A) *Product Profile: 5′ DNA Terminus Labelling System*, Bethesda Research Laboratories, Gaithersburg, MD.

Bethesda Research Laboratories (undated B) *T4 DNA Polymerase*, Bethesda Research Laboratories, Gaithersburg, MD.

Blair, D. G. R. (1985) *Int. J. Biochem. 17*, 23–30.

Blankenship, J., & Walle, T. (1977) *Arch. Biochem. Biophys. 179*, 235–242.

Blankenship, J., & Walle, T. (1978) in *Advances in Polyamine Research* (Campbell, R. A., et al., Eds.) Vol. 2, pp 97–110, Raven Press, New York.

Blankenship, J., & Marchant, P. (1984) *Proc. Soc. Exp. Biol. Med. 177*, 180–187.

Bloomfield, V. A., & Wilson, R. W. (1981) in *Polyamines in Biology & Medicine* (Morris, R. D., & Marton, L. J., Eds.) pp 183–206, Marcel Dekker, New York.

Bohm, L., & Crane-Robinson, C. (1984) *Biosci. Rep. 4*, 365–386.
Braunlin, W. H., Strick, T. J., & Record, M. T., Jr. (1982) *Biopolymers 21*, 1301–1314.
Celano, P., Baylin, S. B., Giardiello, F. M., Nelkin, B. D., & Casero, R. A., Jr. (1988) *J. Biol. Chem. 263*, 5491–5494.
Cotton, R. W., & Hamkalo, B. A. (1981) *Nucleic Acids Res. 9*, 445–457.
DePamphilis, M. L., & Wassarman, P. M. (1980) *Annu. Rev. Biochem. 49*, 627–666.
Doetsch, P. W., Chan, G. L., & Haseltine, W. A. (1985) *Nucleic Acids Res. 13*, 3285–3304.
Drew, H. R., & Dickerson, R. E. (1981) *J. Mol. Biol. 151*, 535–556.
Dumuis-Kervabon, A., Encontre, I., Etienne, G., Jaureguiadell, J., Mery, J., Mesnier, D., & Parello, J. (1986) *EMBO J. 5*, 1735–1742.
Eickbush, T. H., & Moudrianakis, E. N. (1978) *Biochemistry 17*, 4955–4964.
Feuerstein, B. G., Pattabiraman, N., & Marton, L. J. (1986) *Proc. Natl. Acad. Sci. U.S.A. 83*, 5948–5952.
Gale, J. M., Nissen, K. A., & Smerdon, M. J. (1987) *Proc. Natl. Acad. Sci. U.S.A. 84*, 6644–6648.
Garrard, W. T., Cockerill, P. N., Hunting, D. W., McDaniel-Gerwig, D., Szent-Gyorgyi, C., Xu, M., & Gross, D. S. (1988) in *Chromosomes and Chromatin* (Adolph, K. W., Ed.) Vol. I, pp 133–178, CRC Press, Boca Raton, FL.
Godfrey, J. E., Eickbush, T. H., & Moudrianakis, E. N. (1980) *Biochemistry 19*, 1339–1346.
Hebbes, T. R., Thorne, A. W., & Crane-Robinson, C. (1988) *EMBO J. 7*, 1395–1402.
Hirschman, S. Z., Leng, M., & Felsenfeld, G. (1967) *Biopolymers 5*, 227–233.
Janne, J., Pogo, H., & Raina, A. (1978) *Biochem. Biophys. Acta 473*, 241–293.
Libby, P. R. (1978) *J. Biol. Chem. 253*, 233–237.
Libby, P. R. (1980) *Arch. Biochem. Biophys. 203*, 384–389.
Liquori, A. M., Costantino, L., Crescenzi, V., Elia, V., Giglio, E., Puliti, R., DeSantis Savino, M., & Vitagliano, V. (1967) *J. Mol. Biol. 24*, 113–122.
Lutter, L. C. (1979) *Nucleic Acids Res. 6*, 41–56.
Marchant, P. G., & Blankenship, J. (1983) *Proc. West. Pharmacol. Soc. 26*, 65–68.
Marchant, P., Dredar, S., Manneh, V., AlShabanah, O., Matthews, H. R., Fries, D., & Blankenship, J. (1989) *Arch. Biochem. Biophys.* (in press).
Marquet, R., & Houssier, C. (1988) *Biochem. Pharmacol. 37*, 1857–1858.
Matthews, H. R. (1988) in *Chromosomes and Chromatin* (Adolph, K. W., Ed.) Vol. I, pp 3–32, CRC Press, Boca Raton, FL.
Maxam, A. M., & Gilbert, W. (1980) *Methods Enzymol. 65*, 499–560.
McCormick, F. (1978) in *Advances in Polyamine Research* (Campbell, R. A., et al., Eds.) Vol. 1, pp 173–179, Raven Press, New York.
Mocz, G., & Balint, M. (1984) *Anal. Biochem. 143*, 283–292.
Mokrasch, L. C. (1967) *Anal. Biochem. 18*, 64–71.
Morgan, J. E. (1988) Ph.D. Thesis, University of California, Davis.
Morgan, J. E., Blankenship, J. W., & Matthews, H. R. (1986) *Arch. Biochem. Biophys. 246*, 225–232.
Morgan, J. E., Blankenship, J. W., & Matthews, H. R. (1987) *Biochemistry 26*, 3643–3649.
Morse, R. H., & Simpson, R. T. (1988) *Cell 54*, 285–287.
Nagarajan, S., Ganem, B., & Pegg, A. E. (1988) *Biochem. J. 254*, 373–378.
Nielsen, P. E. (1985) *Biochemistry 24*, 2298–2303.
Pegg, A. E. (1986) *Biochem. J. 234*, 249–262.
Pegg, A. E., & McCann, P. P. (1982) *Cell Physiol. 12*, c212–c221.
Pegg, A. E., & McCann, P. P. (1988) *ISI Atlas Sci.: Biochem. 1*, 11–18.
Porschke, D. (1984) *Biochemistry 23*, 4821–4828.
Prunell, A., Kornberg, R. D., Lutter, L., Klug, A., Levitt, M., & Crick, F. H. C. (1979) *Science 204*, 855–858.
Reeves, R. (1988) in *Chromosomes and Chromatin* (Adolph, K. W., Ed.) Vol. I, pp 109–131, CRC Press, Boca Raton, FL.
Richmond, T. J., Finch, J. T., Rushton, B., Rhodes, D., & Klug, A. (1984) *Nature 311*, 532–537.
Rubin, R. L. (1977) *J. Bacteriol. 129*, 916–925.
Seiler, N. (1987) *Can. J. Physiol. Pharmacol. 65*, 2024–2035.
Seiler, N., & Knogden, B. (1980) *J. Chromatogr. 221*, 227–235.
Seiler, N., Bolkenious, F. N., & Rennert, O. M. (1981) *Med. Biol. 59*, 334–346.
Sen, D. S., & Crothers, D. M. (1986) *Biochemistry 25*, 1495–1503.
Simpson, R. T., & Whitlock, J. P. (1976) *Cell 9*, 347–353.
Staros, J. V., Bayley, H., Standring, D. N., & Knowles, J. R. (1978) *Biochem. Biophys. Res. Commun. 80*, 568–572.
Stevens, L. (1967) *Biochem. J. 103*, 811–815.
Stewart, K. D. (1988) *Biochem. Biophys. Res. Commun. 152*, 1441–1446.
Tabor, C. W., & Tabor, H. (1976) *Annu. Rev. Biochem. 45*, 285–306.
Tabor, C. W., & Tabor, H. (1984) *Annu. Rev. Biochem. 53*, 749–790.
Thomas, T. J., & Bloomfield, V. A. (1984) *Biopolymers 23*, 1295–1306.
Thomas, T. J., Bloomfield, V. A., & Canellakis, Z. Z. (1985) *Biopolymers 24*, 725–729.
Trifonov, E. N. (1984) *CRC Crit. Rev. Biochem. 19*, 89–106.
Tsuji, M., Nakajima, T., & Sano, I. (1975) *Clin. Chim. Acta 59*, 161–167.
Wemmer, D. E., Srivenugopal, K. S., Reid, B. R., & Morris, D. R. (1985) *J. Mol. Biol. 185*, 457–459.
Whitlock, J. P., & Simpson, R. T. (1977) *J. Biol. Chem. 252*, 6516–6520.
Zakrewska, K., & Pullman, B. (1986) *Biopolymers 25*, 375–392.